

Evaluation of continuous and discrete melting endotherms for determination of structural heterogeneities in Ziegler-Natta catalyzed linear low density polyethylene

Mostafa Ahmadi^{1*}, Seyed Mohammad Mehdi Mortazavi², Saeid Ahmadjo², Majid Zahmati³, Khosrow Valieghbal³, Davoud Jafarifar³, Reza Rashedi^{1,3}

¹Department of Polymer Engineering and Color Technology, Amirkabir University of Technology, Tehran, Iran.

²Polymerization Engineering Department, Iran Polymer and Petrochemical Institute, Tehran, Iran.

³Central laboratory, Research and development, Jam Petrochemical Company.

Received: 22 January 2016, Accepted: 6 April 2016

ABSTRACT

Ethylene / 1-butene copolymers at different comonomer levels were synthesized using a Ziegler-Natta catalyst to evaluate the applicability of thermal fractionation methods in predicting chemical composition distribution (CCD). The continuous melting endotherms obtained using DSC were converted to continuous CCD, and the average comonomer contents were compared with the NMR results. DSC underestimated the comonomer content specifically at higher levels and demonstrated that it was more sensitive to the chosen baseline. The thermally fractionated melting endotherms by using the SSA method were deconvoluted and transformed to discrete CCDs. The SSA method underestimated the average comonomer content even more than those obtained by DSC, nevertheless its results were more reproducible. The main shortcoming of the thermal methods was the inability of short ethylene sequences in forming discernible lamella thicknesses at high comonomer levels. Calibration curves were created for converting the predicted comonomer contents into the absolute values and used for studying industrial LLDPEs with different comonomer levels. It was shown that SSA provided more reliable results and correlated more reasonably to the measured densities. **Polyolefins J (2016) 3: 135-146**

Keywords: Chemical composition distribution; lamella thickness; short chain branching; thermal fractionation; linear low density polyethylene; Ziegler-Natta catalyst

INTRODUCTION

Polyolefins are the most widely produced polymers due to the cheapness of their raw materials and the high flexibility in tuning their microstructure to attain desired properties. Short chain branching as one of the key factors is utilized in the commercial production of linear low density polyethylene (LLDPE), through incorporation of α -olefin comonomers [1], for example

1-butene, 1-hexene, and 1-octene, to change the crystalline structure and therefore the corresponding properties such as melting and crystallization temperatures [2], as well as the mechanical properties including tensile modulus [3,4]. Hence, determination of different aspects of comonomer enchainment in industrial plants is of great importance not only for controlling the final properties but also for evaluating structure-properties relationships [3,4].

* Corresponding Author - E-mail: mo.ahmadi@aut.ac.ir

The direct method of evaluation of chemical composition distribution (CCD) is physical separation of chains from solution based on their melting and crystallization temperatures as utilized in temperature rising elution fractionation (TREF) and crystallization fractionation analysis (Crystaf), respectively [5]. The latest technology of crystallization elution fractionation (CEF) combines the separation by crystallization and by melting that provides a better resolution of chains having different levels of comonomer contents in significantly shorter times [6]. Cross-fractionation of chains based on comonomer content by TREF and the subsequent assessment of each fraction can provide an enlightening detailed image from the distribution manner of comonomers among chains and its effect on the final properties [7-9]. However, despite all informative results obtained from these methods, they are not widely used in industrial plants since the long measurement time and use of high-temperature solvation make them too expensive for routine use.

Nuclear magnetic resonance (NMR) can provide precise information on average chemical composition but still needs high-temperature solvation and suffers from long acquisition times and maintenance expenses. Fourier transformation infrared (FTIR) is a widely used alternative method for determination of average comonomer content with acceptable accuracy for industrial LLDPE plants. For instance, absorption at 769 cm^{-1} , assigned to the ethyl branches and normalized by the sample film's thickness, is used for determination of 1-butene content [10,11]. However the accuracy and reliability of this method is not extensively studied.

Thermal fractionation by employing carefully designed thermal cycles in differential scanning calorimetry (DSC) offers a quick and practical way to evaluate not only the average but distribution of short chain branching in LLDPEs [12]. Among different fractionation algorithms, successive self-nucleation and annealing (SSA) has been proven to have the most separation resolution [12]. Since the fractionation is not physical, the final results are sensitive to both inter- and intra-molecular heterogeneities, opposed to the physical separation methods such as TREF that assess inter-molecular variations. Through thermal fractionation of different TREF fractions, it has been shown

that single-site metallocene catalysts produce intramolecular heterogeneity while multi-site Ziegler-Natta catalysts generate chains with both inter- and intramolecular comonomer distributions [7,13,14].

There are two distinct regimes of thermal behavior in LLDPEs depending on the amount of comonomer content [15]. From one hand, chain folding in long enough ethylene sequences provides a constant lamella thickness, which is a compromise of kinetics and thermodynamics aspects of crystallization in LLDPEs with low comonomer content. Depending on the measurement conditions, a lamella thickness of about 125 monomer units (or 250 methylene groups) in all-trans conformations is reported for this regime [15]. On the other hand, at higher comonomer levels, exclusion of comonomer side branch from the crystalline cell determines the average lamella thickness, and resulting melting temperature [16]. Thermal fractionation can be used for determination of comonomer content in this regime. Therefore, the minimum detectable molar fraction of comonomer would be 0.8 %. At very high levels of comonomer, on the other hand, the ethylene sequences are not long enough to be able to make packed lamella structures. The crystallization ability vanishes as comonomer content increases and the upper limit of comonomer detection by thermal methods is met.

However, some complicating factors may affect the view mentioned above. There are reports showing that short side branches can be included in the crystalline structures as defects [16,17] or that long side branches may make separate lamellae themselves [18]. Besides, the inter- and intra-molecular comonomer distributions according to Stockmayer and Flory's equations, respectively, [19] broaden the measureable comonomer distribution, and also interfere with the extremes of detectable comonomer contents. The situation becomes significantly complicated in the case of Ziegler-Natta catalysts having multiple active centers with distinct comonomer responses [20].

Since thermal fractionation can be considered as a simpler alternative to physical separation methods for determination of CCD or other heterogeneities, many researchers have compared or combined these methods [21-24]. There are plenty of reports on many different samples made by different catalysts, comono-

nomers, and especially industrial samples from different technologies [13,14,21-24]. Although trends are similar, absolute results are not comparable due to the mentioned differences. Therefore, it would be of practical importance if one could focus on a unique set of copolymers and evaluate the applicability of thermal fractionation methods for determination of microstructure heterogeneities.

In this work, we have synthesized ethylene /1-butene copolymers with different levels of comonomer, using Ziegler-Natta catalyst, and evaluated their microstructure distribution using thermal fractionation methods. We have calculated lamella thickness, short chain branching (SCB), and comonomer content distributions by continuous and discretized melting endotherms and compared the results with the average values obtained from NMR and FTIR. In this way, we have built calibration curves by thermal methods for prediction of chemical composition and used them for evaluation of industrial samples. We have shown that the thermal fractionation methods offer a quick and sensitive alternative for assessment of microstructure heterogeneities. The paper is designed as follows: After presenting the theoretical basis of calculations, evaluation of thermal properties of the synthesized samples measured by normal DSC and SSA and calibration curves made using NMR results are presented. Then the calibration curves are utilized for analysis of industrial samples and final results are discussed.

EXPERIMENTAL

Materials

Ethylene/1-butene copolymers at five different comonomer levels were synthesized using an industrial Ziegler-Natta catalyst. The mass average comonomer

contents were measured by Carbon-NMR and the results are depicted in Table 1. Details of similar synthesis conditions and characterizations can be found elsewhere [20]. As a general procedure, reactions were carried out in a 1 L stainless steel Buchi reactor using 500 ml of hexane as the reaction media. Triethylaluminum (TEAL) and the catalyst were introduced subsequently, after purging reactor several times by nitrogen and saturation of the media with ethylene. The weighted amount of 1-butene comonomer was directly transferred to the reactor. Subsequently, the temperature of reaction and pressure of hydrogen and ethylene were increased to the desired values one after each other, and the reaction was started by switching the mixer on. Pressure drop was compensated by entering ethylene to the reactor through a mass flow controller. After the desired polymerization time, the reaction was terminated by evacuating the remaining unreacted gases and precipitating the reaction products in methanol.

Characterization

All the DSC results were obtained using a Mettler-Toledo apparatus 823e Module, interfaced to a digital computer installed with Star E 9.01 software (sensor FRS5). The sample was heated from room temperature to 160°C at a rate of 10°C min⁻¹ and remained 10 min to remove the thermal history; followed by cooling to 0°C at the same rate. Finally, the polymer was reheated to 160°C using the same rate. The melting peak and crystallinity were determined according to the results of the final step.

The SSA method was used to analyze the CCD of copolymers using the following procedure [25,26]: The sample was heated to 160°C at the rate of 10°C min⁻¹ and maintained at this temperature for 10 min. The sample was then cooled to ambient temperature at

Table 1. Average lamella thickness, SCB and comonomer fractions determined based on continuous and discrete melting endotherms compared with NMR results.

| Samples | DSC | | | | | SSA | | | | | NMR CC/mass% |
|---------|---------------------|--------|------------------|------------|-------------------------------|---------------------|--------|------------------|------------|-------------------------------|-----------------|
| | \bar{L}/nm | DI_L | \overline{SCB} | DI_{SCB} | $\overline{CC}/\text{mass}\%$ | \bar{L}/nm | DI_L | \overline{SCB} | DI_{SCB} | $\overline{CC}/\text{mass}\%$ | |
| S1 | 10.6 | 1.1 | 11.4 | 1.4 | 4.4 | 8.6 | 1.2 | 10.3 | 1.7 | 4.0 | 3.30 |
| S2 | 9.8 | 1.1 | 14.4 | 1.4 | 5.5 | 7.5 | 1.2 | 13.8 | 1.4 | 5.2 | 6.36 |
| S3 | 8.8 | 1.1 | 17.4 | 1.4 | 6.5 | 7.1 | 1.2 | 15.1 | 1.4 | 5.9 | 8.50 |
| S4 | 8.2 | 1.1 | 21.6 | 1.4 | 8.3 | 6.3 | 1.2 | 18.8 | 1.5 | 6.8 | 11.70 |
| S5 | 7.8 | 1.2 | 24.4 | 1.4 | 9.2 | 5.5 | 1.3 | 24.2 | 1.4 | 8.6 | 13.50 |

the same rate, immediately heated to 140°C and maintained at this temperature for 5 min for annealing. The sample was then cooled to ambient temperature at the same rate and immediately heated to the next annealing step. A temperature step 6°C was applied in experiments. The annealing temperatures covered the range of 38-140°C. Finally, the cooled sample was heated from ambient temperature to 160°C at the rate of 10°C min⁻¹ and melting endotherms were recorded.

RESULTS AND DISCUSSIONS

As described in the introduction, there are many sources of complexities, which necessarily imply to evaluate the efficiency of the thermal fractionation methods which are used for determination of CCD of LLDPEs made by Ziegler-Natta catalysts by means of pre-designed samples. We therefore, synthesized five LLDPE samples using Ziegler-Natta catalysts at different 1-butene levels. The mass fractions of incorporated comonomer, determined by NMR, covered 3.3 to 11 mass% as reported in Table 1.

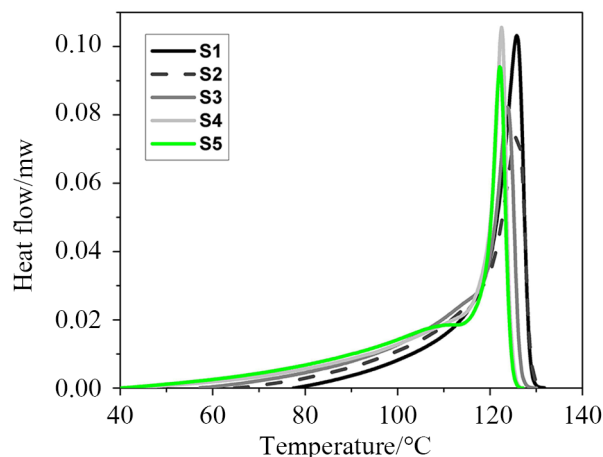
Evaluation of continuous melting endotherms

Figure 1a shows the melting endotherms as measured by normal DSC. The melting peaks shift towards lower temperatures and are broadened on increasing the comonomer content. The continuous melting peaks can be converted to continuous lamella thickness distribution using Gibbs-Thomson equation [18]:

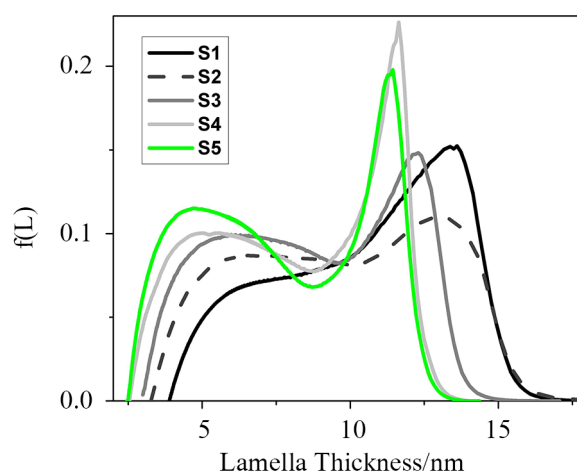
$$T_m = T_m^c \left(1 - \frac{2\sigma_e}{\Delta H_u L_c} \right) \quad (1)$$

where T_m is the melting temperature in the x-axis, stands for equilibrium copolymer melting temperature that depends on comonomer content, $\sigma_e = 0.09 \text{ J m}^{-2}$ is the surface free energy of lamella, $\Delta H_u = 2.96 \times 10^8 \text{ J m}^{-3}$ is the volumetric heat of fusion and L_c is the lamella thickness. Equilibrium melting temperature of a copolymer can be calculated using Flory's Equation [18]:

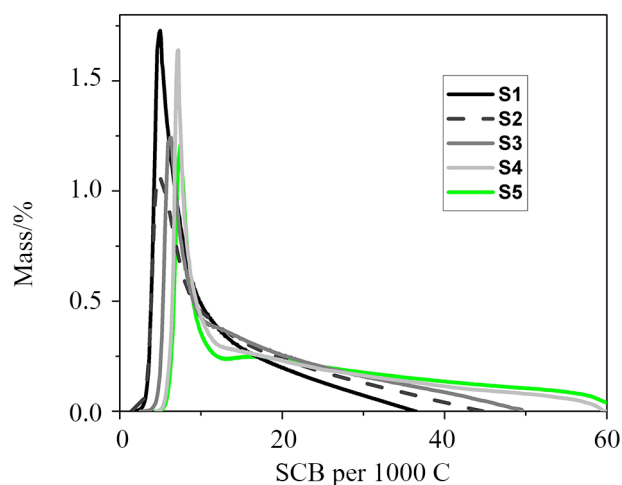
$$\frac{1}{T_m} - \frac{1}{T_m^0} = -\frac{R}{\Delta H} \ln x_a \quad (2)$$



(a)



(b)



(c)

Figure 1. Melting peaks of the synthesized copolymers (a) calculated LTD (b) and calculated distribution of SCB.

where $T_m^0 = 418.6 \text{ K}$ is the equilibrium melting temperature of ethylene homopolymer, $R = 8.314 \text{ J mol}^{-1}$

K^{-1} is the gas constant, and x_a is the mole fraction of crystallizable ethylene sequences along the backbone. The mass fraction of the crystalline lamellae that melt at a specific temperature is related to the melting endotherms through the following differential equation [4]:

$$\frac{1}{M} \frac{dM}{dl} = \frac{dE}{dT} \frac{(T_m^\circ - T_m)^2 \rho_c}{2\sigma_e T_m^\circ M} \quad (3)$$

Where $\rho_c = 1 \text{ g cm}^{-3}$ is the density of crystalline phase, $\frac{1}{M} \frac{dM}{dl}$ represents the population of lamellae ($f(L)$) with the thickness in the range of L and $L+dL$ that melt between T and $T+dT$, and dE/dT is the energy required to melt lamellae, in other words $\frac{1}{M} \frac{dE}{dT}$ is the y-axis divided by the heating rate in $^\circ\text{C min}^{-1}$. The corresponding continuous lamella thickness distribution (LTD) is shown in Figure 1b. The number and length average lamella thickness and its corresponding dispersity index can be calculated using the following equations:

$$\bar{L} = \int_0^\infty Lf(L)dL \quad (4)$$

$$\bar{L}_2 = \frac{\int_0^\infty L^2 f(L)dL}{\int_0^\infty Lf(L)dL} \quad (5)$$

$$DI_L = \frac{\bar{L}_2}{\bar{L}} \quad (6)$$

The average lamella thickness decreases by increasing the comonomer content, as expected, and the dispersity indices increase slightly as shown in Table 1.

The continuous melting peaks can be used to calculate the continuous distribution of SCB per 1000 carbon atoms, as well [27]. Two methods have been used in this regard. Hosoda analyzed TREF fractions to propose empirical relationships between SCB, melting temperature and crystallinity (X_c) for ethylene/1-butene copolymers [28,29]:

$$T_m = -1.55 \text{ SCB} + 134 \quad (7)$$

$$X_c = -0.0132 \text{ SCB} + 0.82 \quad (8)$$

Others used normal alkanes with different lengths to build up such a correlation [16,30]. Both the methods

follow the same trend, however, Hosoda's equation predicts a slightly higher SCB at similar melting temperature. The abscissa of the continuous melting endotherms were transformed into SCB using Equation 7, while the ordinates were divided by the X_c from Equation 8 to account for both the crystalline as well as the amorphous part of the sample at each temperature (not seen in the DSC endotherms). The resultant SCB distributions are shown in Figure 1c. The corresponding averages and dispersity indices were calculated by equations similar to equations 4 to 6, and the results are depicted in Table 1. The SCB distribution can be converted to CCD using the following equations:

$$CC(\text{mol}\%) = 1 - \frac{1000 - i\text{SCB}}{1000 - (i - 2)\text{SCB}} \quad (9)$$

$$CC(\text{mass}\%) = \frac{14iCC(\text{mol}\%)}{28(1 - CC(\text{mol}\%)) + 14iCC(\text{mol}\%)} \quad (10)$$

where CC and i stand for comonomer content and the number of carbon atoms in the comonomer which is four for 1-butene. The mass average comonomer content and the corresponding dispersity index were calculated following Equations 4 to 6 and the results are reported in Table 1. Apparently, the DSC method overestimates comonomer content for the lowest comonomer level and underestimates comonomer content at higher levels [23]. The overestimation at lower comonomer levels is expected considering the fact that the thermal methods reflect at least 0.8 mol% comonomer content for chains containing no comonomers. Besides, the DSC results are extremely sensitive to the choice of baseline; at lower comonomer levels, extra drawn baseline toward lower melting temperature may be the cause of over estimation in the predicted comonomer content that is the case at higher comonomer contents in an opposite manner.

Evaluation of discrete melting endotherms

Thermal fractionation of chains in groups with similar lamella thickness may help to solve the problem of baseline. Therefore, the samples were fractionated using the SSA method in groups separated by 6°C . Standard Gaussian distribution function was used to deconvolute the final endotherms into the weighted summation of several peaks, and the results are shown

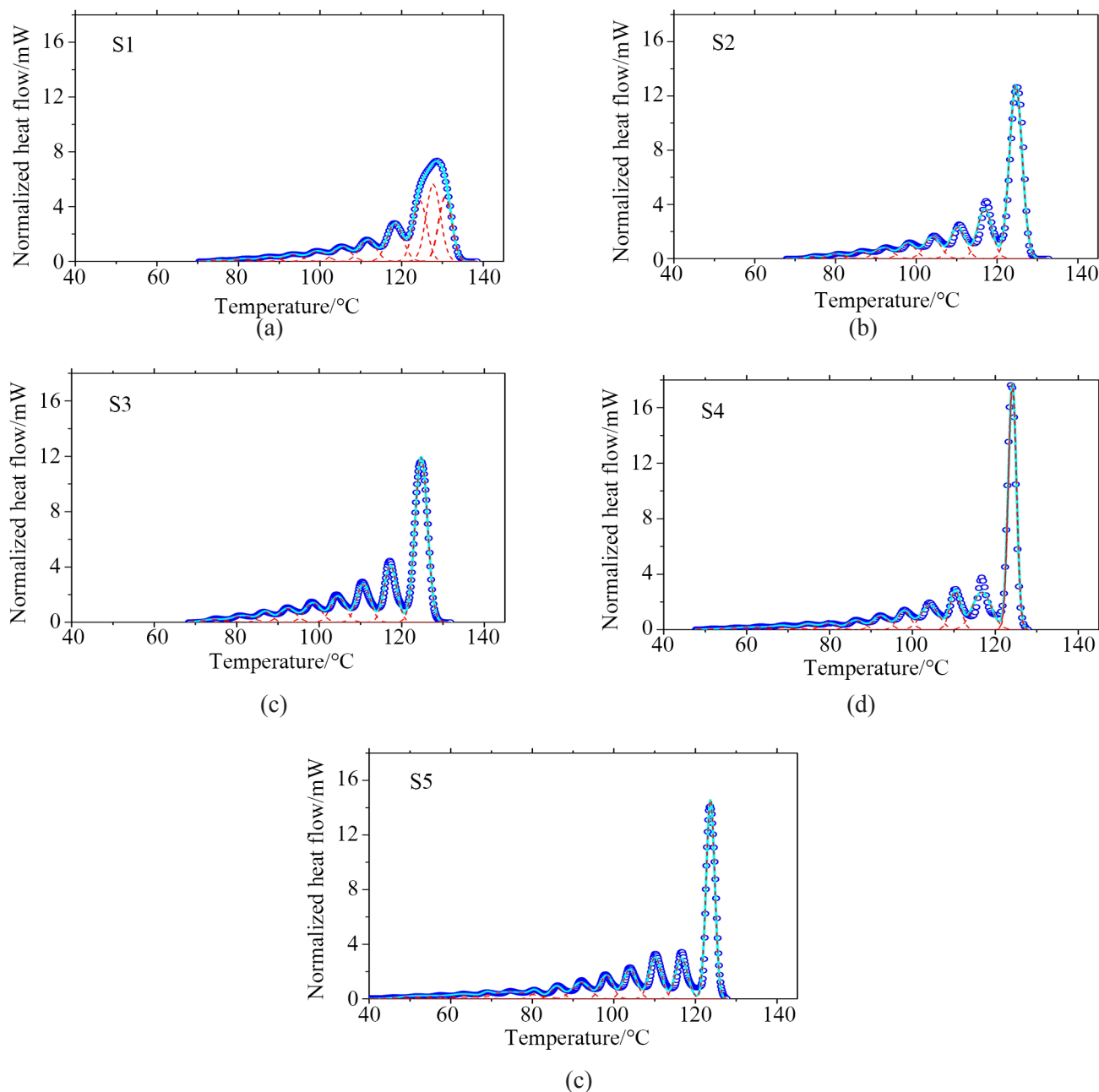


Figure 2. Deconvolution of SSA graphs into several standard Gaussian distributions.

in Figure 2. Normalized error was defined to obtain a similar precision on both high and low temperature regions [25,26].

The population of the chains melting at higher temperatures decreases and the population of the chains melting at lower temperatures increases as the comonomer content increases (Figure 3a). Equations 1 to 8 were used to create the discrete distributions of lamellae thickness and SCB per 1000 carbon atoms as shown in Figures 3b and 3c, and the corresponding average and dispersity indices are reported in Table 1.

As can be seen in Table 1, the SSA method follows the same trend already reported for the DSC results, however, it underestimates comonomer content at higher levels even further. The main reason is the fact that the chains with higher comonomer levels exhibit a very low crystallization ability and do not form detectable contributions specially while are fractionated into separate groups. The SSA results are more reproducible, since the choice of baseline is less arbitrary.

The aforementioned complications make the thermal methods somewhat inaccurate, despite their sen-

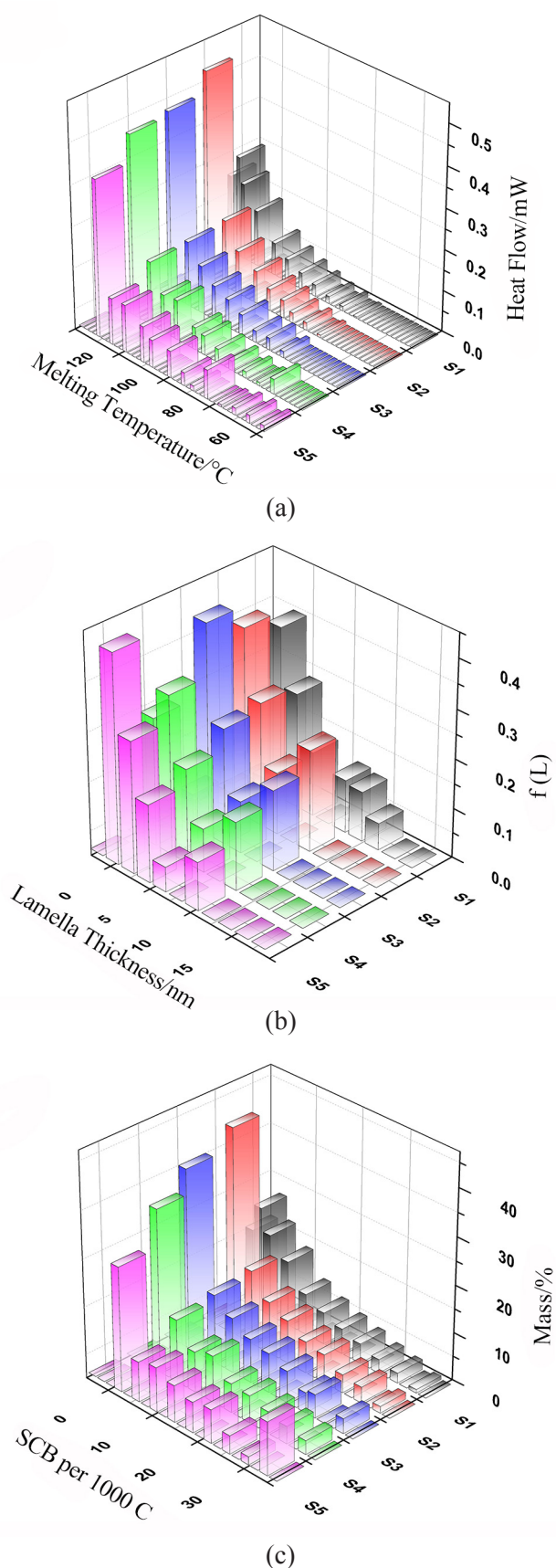


Figure 3. Discrete melting peaks of the synthesized copolymers (a) discrete distributions of lamella thickness (b) and SCB per 1000 carbon atoms (c).

sitivity. Hence, the calibration curves were created to predict the absolute comonomer contents based on the NMR data obtained (the last column of Table 1) and the results are shown in Figure 4. It should be emphasized that we selected the simplest calibration curve based on linear regression in order to keep the generality and extensibility of the predictions out of the measured comonomer content range.

As explained before, since the thermal methods are expected to detect at least 0.8 mole% (equal to 1.6 mass%) 1-butene for linear ethylene homopolymer, the calibration curves are built by adding the corresponding point to the experimental data. In this way, the measured values between 0 and ~2 mass% return negative values by applying the calibration curve, which should be regarded as zero.

Application of both methods on the unknown industrial samples

The obtained calibration curves can be generally used for Ziegler-Natta derived ethylene/1-butene copolymers in the studied range of chemical compositions. Examples are described as follows: Three industrial LLDPE grades with different comonomer levels were produced in two gas phase reactors in series, using two different catalysts; the original and the substituent catalysts, hereafter denoted as Catalyst 1 and Catalyst 2, respectively. The main process conditions in the successive reactors, represented by R1 and R2, are compared in Table 2. While sample HD is essentially high density polyethylene with no comonomer, samples LL1 and LL2 are LLDPEs with distinctly different comonomer levels.

Melting peaks of the industrial LLDPEs are compared in Figure 5a. By increasing comonomer level in the reactors there is a clear shift of the whole melting endotherms towards lower temperatures with increasing tail at lower temperatures. Similar trends are observable in the corresponding LTDs and distributions of SCB created using Equations 1 to 10, as shown in Figures 5b and 5c. The corresponding averages are depicted in Table 3. The fifth column shows the mass fraction of comonomer calculated using the calibration curve obtained for the DSC results in Figure 4. The DSC method clearly overestimates the comonomer content, as predicted particularly about 2 mass%

Table 2. Operation conditions for production of industrial LL-DPEs in series gas phase reactors.

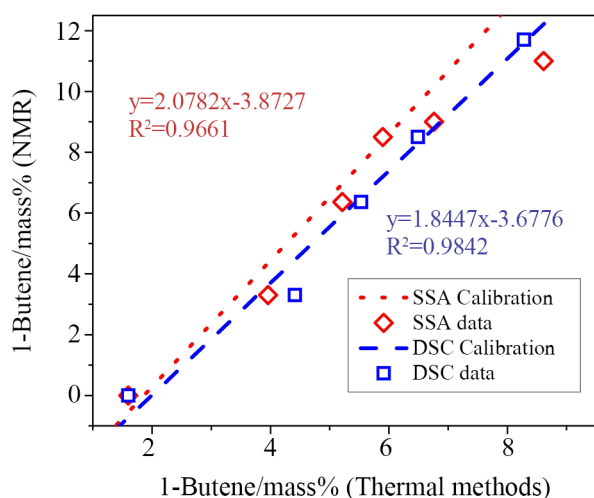
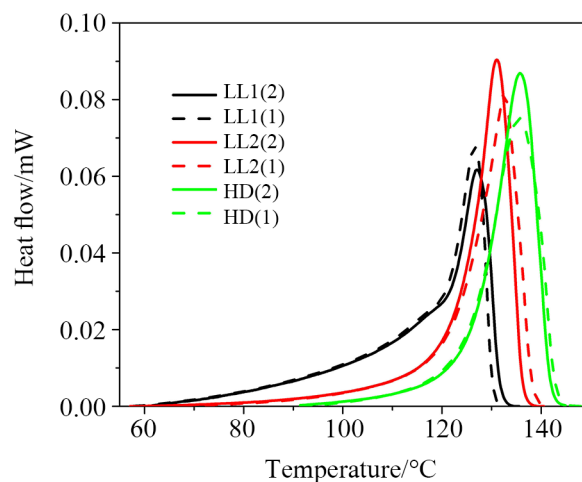
| Sample | T/°C | | P/bar | | H ₂ /C ₂ ^(a) | | C ₄ /mass% ^(b) | |
|--------|----------------|----------------|----------------|----------------|---|----------------|--------------------------------------|----------------|
| | R ₁ | R ₂ | R ₁ | R ₂ | R ₁ | R ₂ | R ₁ | R ₂ |
| LL1 | 75 | 80 | 25 | 25 | 0.26 | 0.32 | 5.75 | 6.25 |
| LL2 | 80 | 85 | 25 | 25 | 0.8 | 0.9 | 1.3 | 1.5 |
| HD | 80 | 85 | 25 | 25 | 0.5 | 0.6 | - | - |

(^a) mole ratio in the reactors, (^b) mass fraction in the reactors

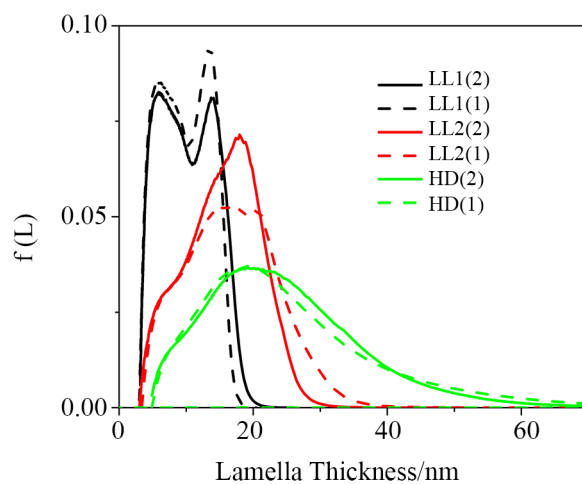
comonomer for the HD samples. Besides, even if there is a difference between the original and the substituent catalysts in comonomer incorporations, the DSC method is unable to detect any discernible differences which are larger than the resolution limit of the measurements.

The SSA method was also used to compare the industrial samples, and the normalized graphs are shown in Figure 6. The difference between samples is more clearly depicted in the SSA results, with increasing population of groups melting at lower temperatures, and decreasing the ones melting at higher temperatures. The graphs were deconvoluted as described before, and the corresponding discrete distribution of melting endotherms, lamella thickness and SCB are compared in Figure 7.

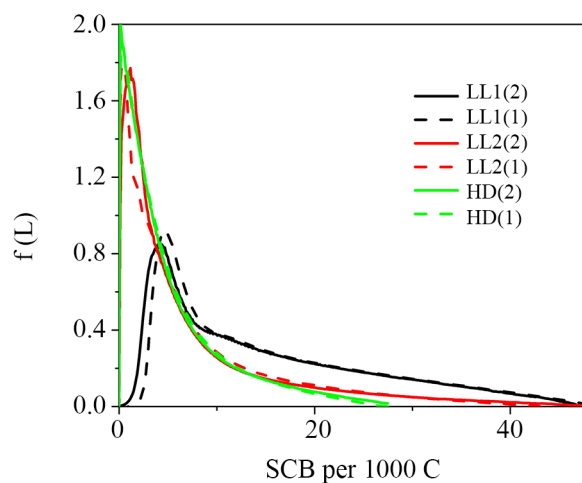
The corresponding averages are shown in Table 3, as well. The ninth column shows the mass fraction of comonomer, calculated using the calibration curve obtained for the SSA method in Figure 4. The SSA method clearly predicts comonomer contents in a more logical manner and the obtained results fol-

**Figure 4.** Calibration curves for prediction of 1-butene mass% based on normal DSC and SSA.

(a)



(b)



(c)

Figure 5. (a) Melting peaks of industrial LLDPEs (b) calculated LTD and (c) calculated distribution of SCB.

low the comonomer fractions in the reactors that are shown in Table 2. Again, the difference between re-

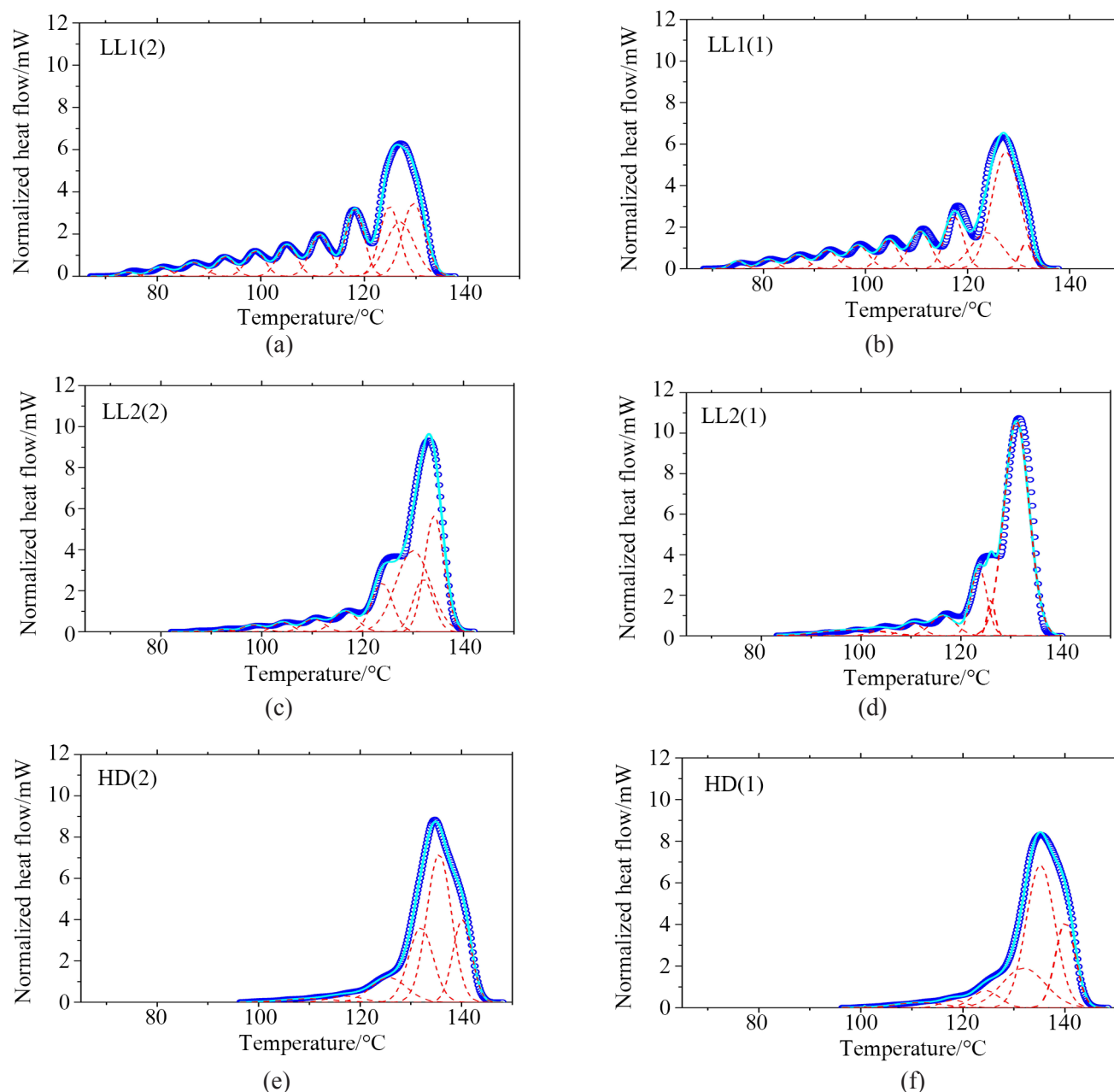


Figure 6. Deconvolution of SSA graphs into several standard Gaussian distributions.

sults obtained for the original and substituent catalysts (also the dispersity indices that are not shown here)

are not significant, except that the substituent may incorporate slightly lower number of comonomer units.

Table 3. Average lamella thickness, SCB and comonomer fractions determined based on continuous and discrete melting endotherms compared with FTIR results and corresponding densities.

| Sample | DSC | | | | SSA | | | | $\overline{CC}/\text{mass\%}$ (FTIR) | Density /g ml ⁻¹ |
|--------|--------------------------|------|-------------------------------|--|--------------------------|------|-------------------------------|--|--------------------------------------|-----------------------------|
| | \overline{L}/nm | SCB | $\overline{CC}/\text{mass\%}$ | $\overline{CC}/\text{mass\%}$ (Calib.) | \overline{L}/nm | SCB | $\overline{CC}/\text{mass\%}$ | $\overline{CC}/\text{mass\%}$ (Calib.) | | |
| LL1(2) | 10.2 | 15.4 | 5.9 | 7.2 | 7.6 | 13 | 5 | 6.5 | 6.6 | 0.923 |
| LL1(1) | 9.9 | 15.7 | 6 | 7.4 | 7.5 | 13.2 | 5.1 | 6.7 | 6.5 | 0.922 |
| LL2(2) | 15.7 | 6.9 | 2.7 | 1.3 | 12.3 | 4.6 | 1.8 | 0 | <1.5 | 0.952 |
| LL2(1) | 17.1 | 7.1 | 2.8 | 1.5 | 11.2 | 5.8 | 2.3 | 0.9 | <1.5 | 0.952 |
| HD(2) | 25.5 | 4.6 | 1.8 | 0 | 17.1 | 1.8 | 0.7 | 0 | <1.5 | 0.959 |
| HD(1) | 27 | 5 | 2 | 0 | 17.6 | 1.6 | 0.6 | 0 | <1.5 | 0.96 |

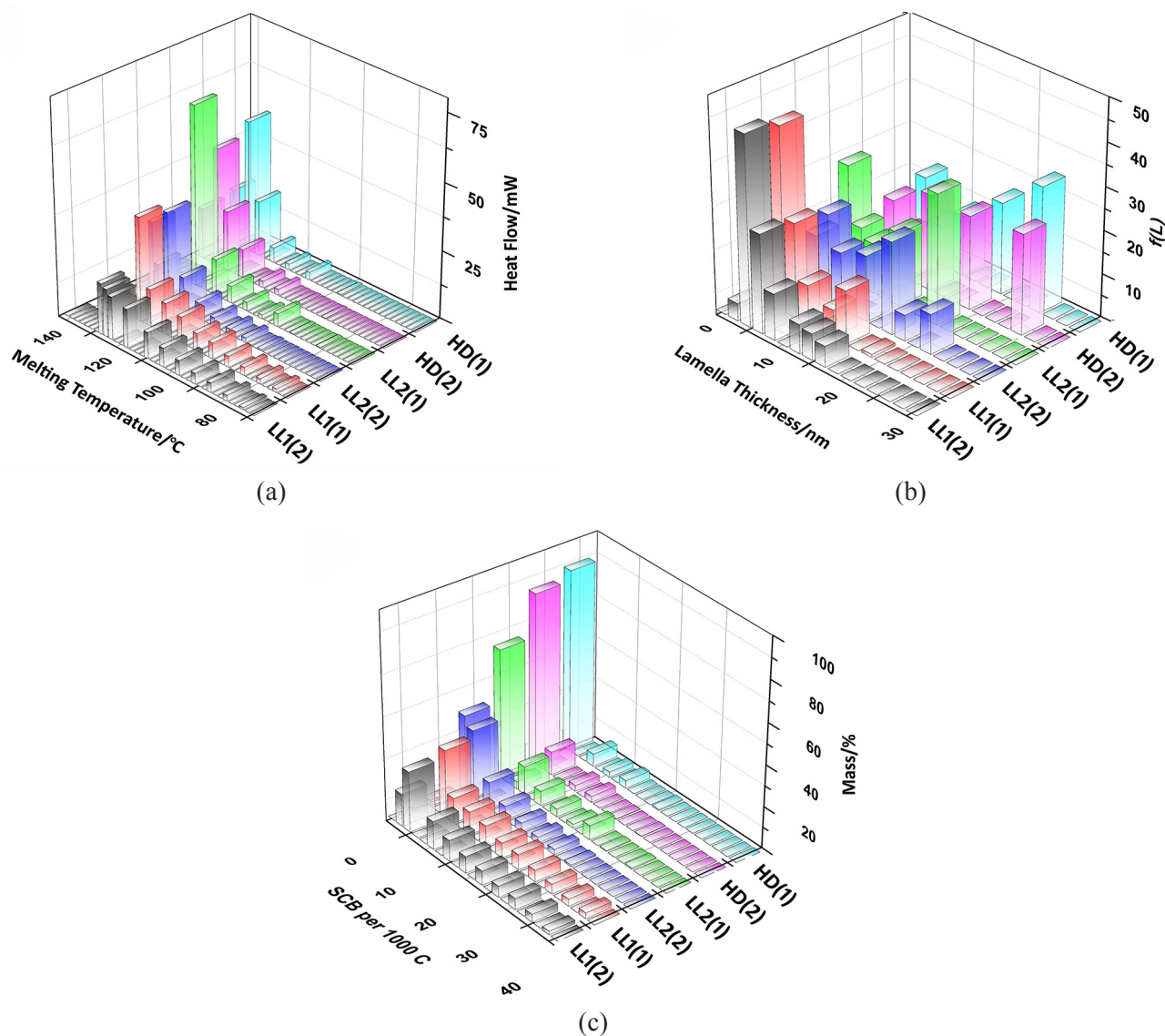


Figure 7. Discrete melting peaks of the industrial copolymers (a) discrete distributions of lamella thickness (b) and SCB per 1000 carbon atoms (c).

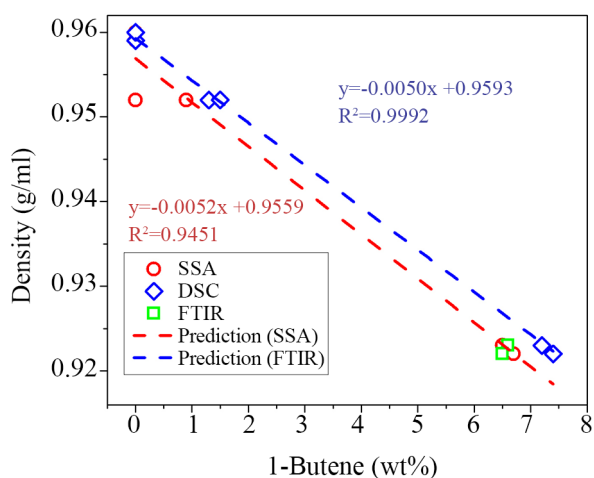


Figure 8. Correlations of the measured densities with 1-butene (mass%) predicted using FTIR, DSC and SSA methods.

Such a difference could be better elucidated using cross fractionation based on molecular mass as well as comonomer content [9].

As described before, FTIR is usually used as a quick alternative for evaluation of comonomer content in industrial plants [10,11]. The comonomer values, as reported by the industrial lab on a daily measurement basis, are depicted in the tenth column of Table 3. It is clear that the specifically defined FTIR method is unable to resolve samples having comonomer contents below 1.5 mass%. Therefore the LLDPE samples with lower 1-butene fractions cannot be distinguished using FTIR, while the SSA and DSC methods both provide more sensitive results. The last column in Table 3 provides the density values as reported by the in-

dustrial lab. The correlation between density values and predicted comonomer contents using the thermal methods and FTIR are compared in Figure 8. Both DSC and SSA results show linear correlations with density, but the SSA method with the prediction of comonomer content reasonably can be considered as a more reliable alternative.

CONCLUSION

Ziegler-Natta catalysts create polydisperse chains with inter- and intra-molecular comonomer distributions and this specificity is exaggerated by the multiple-site nature of these catalysts. We evaluated application of continuous melting endotherms and the fractionated ones based on the SSA method in studying comonomer content and its distribution in this class of polyolefins. Several ethylene/1-butene copolymers were synthesized using Ziegler-Natta catalyst at different comonomer levels. The continuous melting endotherms were converted to LTD, distribution of SCB and CCD, and the average comonomer contents were compared with the NMR results. It was shown that, DSC underestimated comonomer contents specifically at higher levels. The thermally fractionated melting endotherms were deconvoluted and transformed into discrete LTD, distribution of SCB and CCD. The SSA method, despite being more reproducible, also underestimated the average comonomer content even more than DSC. The main shortcoming of the thermal methods at high comonomer contents was the inability of short ethylene sequences in forming discernible lamella thickness. Calibration curves were therefore created to convert the predicted comonomer contents into absolute values. The calibration curves were used for studying CCD in industrial LLDPEs with different comonomer levels. It was confirmed that SSA could provide more reasonable comonomer contents that correlated more reliably to the measured densities.

REFERENCES

1. Khorasani MM, Saeb MR, Mohammadi Y, Ahmadi M (2014) The evolutionary development of chain

microstructure during tandem polymerization of ethylene: A Monte Carlo simulation study. *Chem Eng Sci* 111: 211-219

2. Saeb MR, Mohammadi Y, Ahmadi M, Khorasani MM, Stadler FJ (2015) A Monte Carlo-based feeding policy for tailoring microstructure of copolymer chains: Reconsidering the conventional metallocene catalyzed polymerization of α -olefins. *Chem Eng J* 274: 169-180
3. Zahedi M, Ahmadi M, Nekoomanesh M (2008) Influence of molecular mass distribution on flow properties of commercial polyolefins. *J Appl Polym Sci* 108: 3565-3571
4. Zahedi M, Ahmadi M, Nekoomanesh M (2008) Influence of microstructure and morphology on stress-strain behavior of commercial high density polyethylene. *J Appl Polym Sci* 110: 624-631
5. Pasch H, Malik MI, Macko T (2013) Recent advances in high-temperature fractionation of polyolefins. *Adv Polym Sci* 251: 77-140
6. Monrabal B, Sancho-Tello J, Mayo N, Romero L (2007) Crystallization elution fractionation. A new separation process for polyolefin resins. *Macromol Symp* 257: 71-79
7. Zhang M, Lynch DT, Wanke SE (2000) Characterization of commercial LLDPE by TREF-DSC and TREF-SEC cross-fractionation. *J Appl Polym Sci* 75: 960-967
8. Kebritchi A, Nekoomansh M, Mohammadi F, Khonakdar HA. (2015) The ablative behavior of high linear chains and its role in the thermal stability of polyethylene: A combined P-TREF-TGA study. *Polym Int* 64: 1316-1325
9. Yau WW (2007) Examples of using 3D-GPC-TREF for polyolefin characterization. *Macromol Symp* 257: 29-45
10. Blitz JP, McFaddin DC (1994) The characterization of short chain branching in polyethylene using fourier transform infrared spectroscopy. *J Appl Polym Sci* 11: 13-20
11. Mahdavi H, Enayati Nook M (2008) Characterization and microstructure study of low-density polyethylene by fourier transform infrared spectroscopy and temperature rising elution fractionation. *J Appl Polym Sci* 109: 3492-3501

12. Müller AJ, Michell RM, Pérez RA, Lorenzo AT (2015) Successive self-nucleation and annealing (SSA): Correct design of thermal protocol and applications. *Eur Polym J* 65:132-154
13. Mortazavi SMM, Jafarian H, Ahmadi M, Ahmadjo S (2016) Characteristics of linear branched polyethylene reactor blends synthesized by metallocene late transitional metal hybrid catalysts. *J Therm Anal Calorim* 123: 1469-1478
14. Zhang M, Lynch DT, Wanke SE (2001) Effect of molecular structure distribution on melting and crystallization behavior of 1-butene/ ethylene copolymers. *Polymer* 42: 3067-3075
15. Kissin YV (2011) Modeling differential scanning calorimetry melting curves of ethylene/ α -olefin copolymers. *J Polym Sci Polym Phys* 49:195-205
16. Piel C, Starck P, Seppala JV, Kaminsky W (2006) Thermal and mechanical analysis of metallocene-catalyzed ethene- α -olefin copolymers: The influence of the length and number of the crystallizing side chains. *J Polym Sci Polym Chem* 44:1600-1612
17. Hosoda S, Nozue Y, Kawashima Y, Suita K, Seno S, Nagamatsu T (2011) Effect of the sequence length distribution on the lamella crystal thickness and thickness distribution of polyethylene: Perfectly equi-sequential ADMET polyethylene vs ethylene/ α -Olefin copolymer. *Macromolecules* 44: 313-319
18. Janicek M, Cermak R, Obadal M, Piel C, Ponizil P (2011) Ethylene copolymers with crystallizable side chains. *Macromolecules* 44: 6759-6766
19. Soares JBP (2007) An overview of important microstructural distributions for polyolefin analysis. *Macromol Symp* 257: 1-12
20. Ahmadi M, Nekoomanesh M, Arabi M (2010) A simplified comprehensive kinetic scheme for modeling of ethylene/1-butene copolymerization using Ziegler-Natta catalysts. *Macromol React Eng* 4: 135-144
21. Matsko A, Vanina MP, Echevskaya LG, Zakharov VA (2013) Study of the compositional heterogeneity of ethylene-1-hexene copolymers by thermal fractionation technique by means of differential scanning calorimetry. *J Therm Anal Calorim* 113: 923-932
22. Chen F, Shanks RA, Amarasinghe G (2004) Molecular distribution analysis of melt-crystallized ethylene copolymers. *Polym Int* 53: 1795-1805
23. Zhang M, Wanke SE (2003) Quantitative determination of short-chain branching content and distribution in commercial polyethylenes by thermally fractionated DSC. *Polym Eng Sci* 43: 1878-1888
24. Zhai YM, Wang Y, Yang W, Xie BH, Yang M (2012) A thermal method for quantitatively determining the content of short chain branching in ethylene/ α -olefin copolymers. *J Therm Anal Calorim* 110: 1389-1394
25. Mortazavi SMM, Arabi H, Zhouri GH, Ahmadjo S, Nekoomanesh M, Ahmadi M (2010) Copolymerization of ethylene using Bis-2PhIndZrCl₂ study of structural comonomer composition distribution. *Polym Int* 59: 1258-1265
26. Mortazavi SMM, Arabi H, Zhouri GH, Ahmadjo S, Nekoomanesh M, Ahmadi M (2009) Ethylene homo- and copolymerization using a bis-IndZrCl₂ metallocene catalyst: Structural composition distribution of the copolymer. *Macromol React Eng* 3: 263-270
27. Torabi SR, Fazeli N (2009) A rapid quantitative method for determination of short chain branching content and branching distribution index in LLDPEs by DSC. *Polym Test* 28: 866-870
28. Hosoda S (1988) Structural distribution of LLDPEs. *Polymer J* 20: 383-397
29. Adisson E, Ribeiro M, Deffieux A, Fontanille M (1992) Evaluation of the heterogeneity in LLDPE co-monomer unit distribution by DSC characterization of thermally treated samples. *Polymer* 33: 4337-4342
30. Keating MY, McCord EF (1994) Evaluation of the comonomer distribution in ethylene copolymers using DSC fractionation. *Thermochim Acta* 243: 129-145